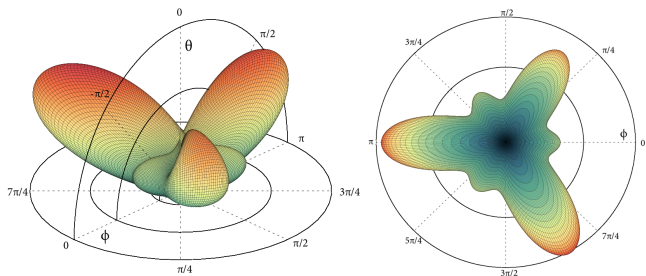


Theoretical Optical Second-Harmonic Calculations for Surfaces

Sean M. Anderson

Centro de Investigaciones en Óptica, A.C

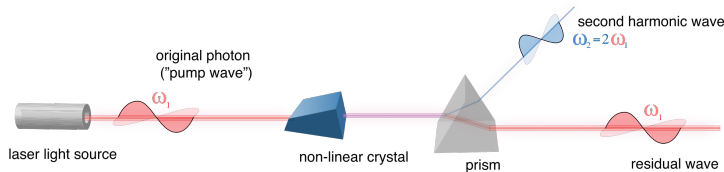
July 14, 2016



Second Harmonic Generation (SHG)

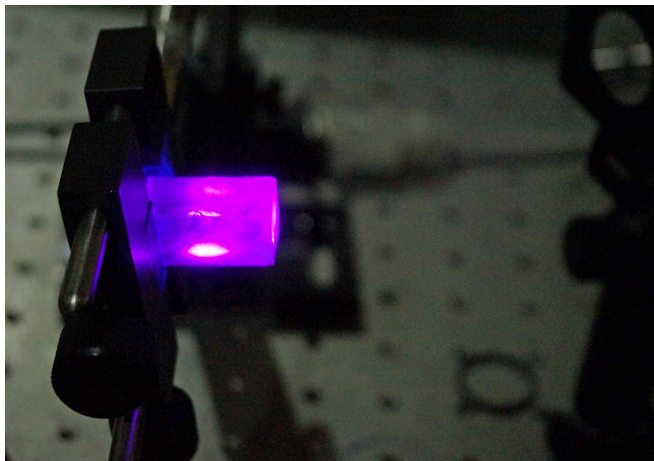
Characteristics¹

- Two photons of the same frequency combine
- Create one photon of double the frequency



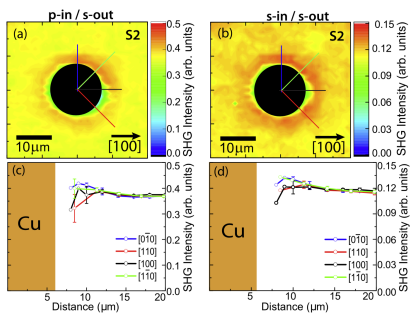
¹Image: Jon Chui

A Nonlinear Crystal

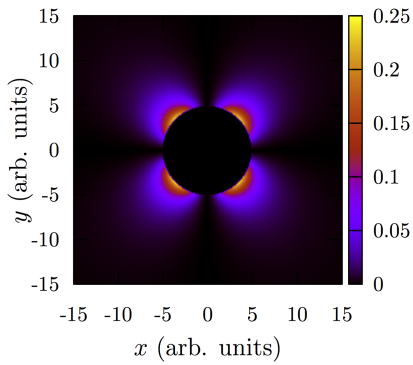


A nonlinear KDP crystal excited at 800 nm, with SHG at 400 nm.

└ Introduction

Applications: Strain in TSVs^{2 3}

Experiment



Theory

² Cho et al., Appl. Phys. Lett. 108, 151602 (2016)³ Mendoza et al., Phys. Status Solidi B 253, 2 (2016)

Second-order Nonlinear Effects

Second-order nonlinear processes^{4 5}

- Are dipole forbidden in the bulk of centrosymmetric materials
- Are related to $\chi^{(2)}$, the nonlinear susceptibility
- Have bigger dipolar (surface) than quadrupolar contributions

Summary

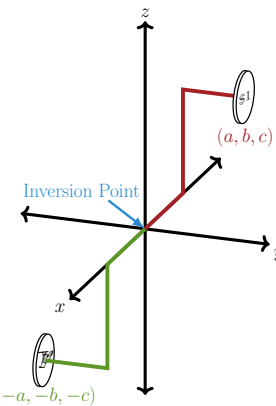
SHG is well suited for studying surfaces and interfaces!

⁴ Armstrong *et al.*, Phys. Rev. 127, 1918 (1962)

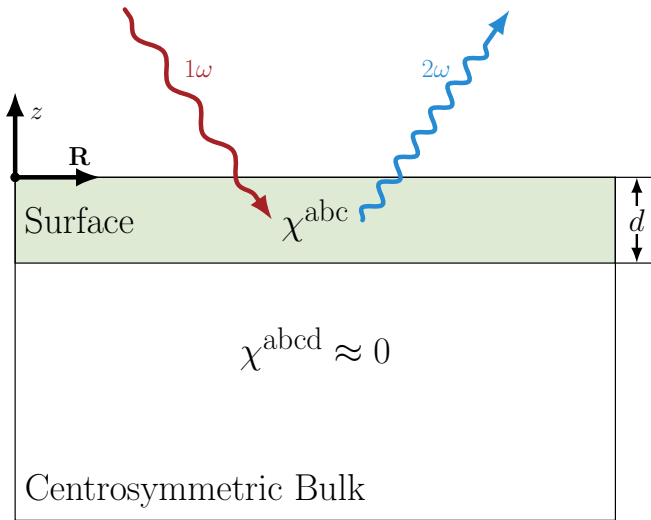
⁵ Bloembergen *et al.*, Phys. Rev. 128, 606 (1962)

Centrosymmetric Materials

A centrosymmetric material is a material that displays inversion symmetry, such that $p(a, b, c) \rightarrow p(-a, -b, -c)$.

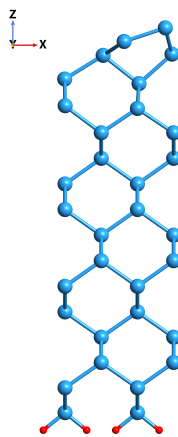


└ Introduction

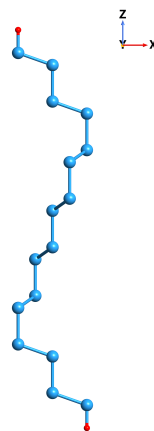


Semi-infinite system with a centrosymmetric bulk and a surface region is of thickness $\sim d$. Dipolar SHG is produced in reflection from the surface.

Two Si Test Cases



Si(001)(2×1)



Si(111)(1×1):H

└ The Nonlinear Surface Susceptibility

 └ Nonlocal Operators

New Contributions to the Theory

Our new formulation adds three contributions (within the IPA):⁶

- 1 The scissors correction
- 2 The contribution from the nonlocal part of the pseudopotential
- 3 The layered cut function

⁶Anderson *et al.*, Phys. Rev. B. 91, 075302 (2015)

- └ The Nonlinear Surface Susceptibility

- └ Nonlocal Operators

Electron Position Operator

We have the electron position operator as

$$\mathbf{r} = \mathbf{r}_i + \mathbf{r}_e,$$

for interband (e) and intraband (i) transitions. The matrix elements of \mathbf{r}_i and \mathbf{r}_e are given by

$$\langle n\mathbf{k}|\mathbf{r}_i|m\mathbf{k}'\rangle = \delta_{nm} [\delta(\mathbf{k} - \mathbf{k}')\xi_{nn}(\mathbf{k}) + i\nabla_{\mathbf{k}}\delta(\mathbf{k} - \mathbf{k}')],$$

$$\langle n\mathbf{k}|\mathbf{r}_e|m\mathbf{k}'\rangle = (1 - \delta_{nm})\delta(\mathbf{k} - \mathbf{k}')\xi_{nm}(\mathbf{k}).$$

- └ The Nonlinear Surface Susceptibility

- └ Nonlocal Operators

Scissors Operator and \mathbf{v}^{nl} (1 & 2)

We express the electron velocity operator as

$$\mathbf{v}^\Sigma = \mathbf{v} + \mathbf{v}^{\text{nl}} + \mathbf{v}^S = \mathbf{v}^{\text{LDA}} + \mathbf{v}^S,$$

where

$$\begin{aligned}\mathbf{v} &= \frac{\mathbf{p}}{m_e}, \\ \mathbf{v}^{\text{nl}} &= \frac{1}{i\hbar} [\mathbf{r}, V^{\text{nl}}], \\ \mathbf{v}^S &= \frac{1}{i\hbar} [\mathbf{r}, S(\mathbf{r}, \mathbf{p})], \\ \mathbf{v}^{\text{LDA}} &= \mathbf{v} + \mathbf{v}^{\text{nl}}.\end{aligned}$$

We also have that

$$\mathbf{r}_{nm}(\mathbf{k}) = \frac{\mathbf{v}_{nm}^\Sigma(\mathbf{k})}{i\omega_{nm}^\Sigma(\mathbf{k})} = \frac{\mathbf{v}_{nm}^{\text{LDA}}(\mathbf{k})}{i\omega_{nm}^{\text{LDA}}(\mathbf{k})}.$$

└ The Nonlinear Surface Susceptibility

 └ Layered Cut Function

Layered Cut Function (3)

We introduce the cut function

$$\mathcal{C}(z) = \Theta(z - z_\ell + \Delta_\ell^b) \Theta(z_\ell - z + \Delta_\ell^f),$$

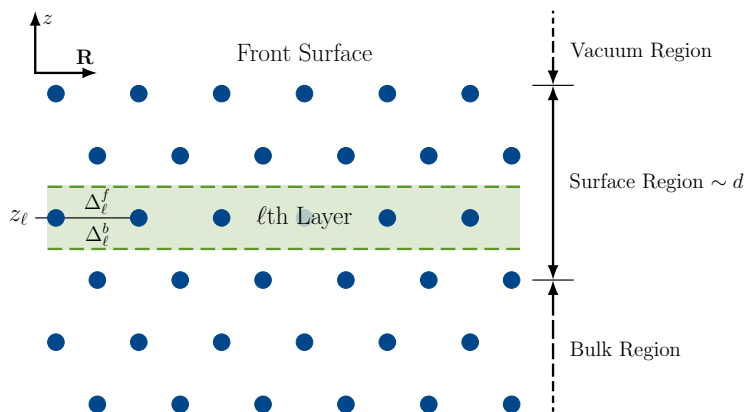
that transforms any operator into its calligraphic counterpart as

$$\mathbf{V} \rightarrow \mathcal{V} = \frac{\mathcal{C}(z)\mathbf{V} + \mathbf{V}\mathcal{C}(z)}{2},$$

└ The Nonlinear Surface Susceptibility

└ Layered Cut Function

Layered Cut Function (3)



Sketch of the super-cell. The atomic slab corresponds to the circles representing the atoms of the system.

└ The Nonlinear Surface Susceptibility

└ Summary

Final Expressions

Interband Contribution $\langle n\mathbf{k}|\mathbf{r}_e|m\mathbf{k}'\rangle = (1 - \delta_{nm})\delta(\mathbf{k} - \mathbf{k}')\xi_{nm}(\mathbf{k})$

$$\text{Im}[\chi_{e,\omega}^{\text{abc}}] = \frac{\pi|e|^3}{2\hbar^2} \int \frac{d^3k}{8\pi^3} \sum_{vc} \sum_{q \neq (v,c)} \frac{1}{\omega_{cv}^\Sigma} \left[\frac{\text{Im}[\mathcal{V}_{qc}^{\Sigma,a}\{r_{cv}^b r_{vq}^c\}]}{(2\omega_{cv}^\Sigma - \omega_{cq}^\Sigma)} - \frac{\text{Im}[\mathcal{V}_{vq}^{\Sigma,a}\{r_{qc}^c r_{cv}^b\}]}{(2\omega_{cv}^\Sigma - \omega_{qv}^\Sigma)} \right] \delta(\omega_{cv}^\Sigma - \omega)$$

$$\text{Im}[\chi_{e,2\omega}^{\text{abc}}] = -\frac{\pi|e|^3}{2\hbar^2} \int \frac{d^3k}{8\pi^3} \sum_{vc} \frac{4}{\omega_{cv}^\Sigma} \left[\sum_{v' \neq v} \frac{\text{Im}[\mathcal{V}_{vc}^{\Sigma,a}\{r_{cv}^b r_{v'v}^c\}]}{2\omega_{cv'}^\Sigma - \omega_{cv}^\Sigma} - \sum_{c' \neq c} \frac{\text{Im}[\mathcal{V}_{vc}^{\Sigma,a}\{r_{cc'}^c r_{c'v}^b\}]}{2\omega_{c'v}^\Sigma - \omega_{cv}^\Sigma} \right] \delta(\omega_{cv}^\Sigma - 2\omega)$$

Intraband Contribution $\langle n\mathbf{k}|\mathbf{r}_i|m\mathbf{k}'\rangle = \delta_{nm} \left[\delta(\mathbf{k} - \mathbf{k}')\xi_{nn}(\mathbf{k}) + i\nabla_{\mathbf{k}}\delta(\mathbf{k} - \mathbf{k}') \right]$

$$\text{Im}[\chi_{i,\omega}^{\text{abc}}] = \frac{\pi|e|^3}{2\hbar^2} \int \frac{d^3k}{8\pi^3} \sum_{cv} \frac{1}{(\omega_{cv}^\Sigma)^2} \left[\text{Re} \left[\left\{ r_{cv}^b (\mathcal{V}_{vc}^{\Sigma,a})_{;k^c} \right\} \right] + \frac{\text{Re} [\mathcal{V}_{vc}^{\Sigma,a} \{r_{cv}^b \Delta_{cv}^c\}]}{\omega_{cv}^\Sigma} \right] \delta(\omega_{cv}^\Sigma - \omega)$$

$$\text{Im}[\chi_{i,2\omega}^{\text{abc}}] = \frac{\pi|e|^3}{2\hbar^2} \int \frac{d^3k}{8\pi^3} \sum_{vc} \frac{4}{(\omega_{cv}^\Sigma)^2} \left[\text{Re} \left[\mathcal{V}_{vc}^{\Sigma,a} \left\{ (r_{cv}^b)_{;k^c} \right\} \right] - \frac{2\text{Re} [\mathcal{V}_{vc}^{\Sigma,a} \{r_{cv}^b \Delta_{cv}^c\}]}{\omega_{cv}^\Sigma} \right] \delta(\omega_{cv}^\Sigma - 2\omega)$$

└ The Nonlinear Surface Susceptibility

└ Summary

Final Expressions

Interband Contribution $\langle n\mathbf{k}|\mathbf{r}_e|m\mathbf{k}'\rangle = (1 - \delta_{nm})\delta(\mathbf{k} - \mathbf{k}')\xi_{nm}(\mathbf{k})$

$$\text{Im}[\chi_{e,\omega}^{\text{abc}}] = \frac{\pi|e|^3}{2\hbar^2} \int \frac{d^3k}{8\pi^3} \sum_{vc} \sum_{\mathbf{q} \neq (v,c)} \frac{1}{\omega_{cv}^\Sigma} \left[\frac{\text{Im}[\mathcal{V}_{\mathbf{q}c}^{\Sigma,a}\{r_{cv}^b r_{v\mathbf{q}}^c\}]}{(2\omega_{cv}^\Sigma - \omega_{c\mathbf{q}}^\Sigma)} - \frac{\text{Im}[\mathcal{V}_{v\mathbf{q}}^{\Sigma,a}\{r_{\mathbf{q}c}^c r_{cv}^b\}]}{(2\omega_{cv}^\Sigma - \omega_{\mathbf{q}v}^\Sigma)} \right] \delta(\omega_{cv}^\Sigma - \omega)$$

$$\text{Im}[\chi_{e,2\omega}^{\text{abc}}] = -\frac{\pi|e|^3}{2\hbar^2} \int \frac{d^3k}{8\pi^3} \sum_{vc} \frac{4}{\omega_{cv}^\Sigma} \left[\sum_{v' \neq v} \frac{\text{Im}[\mathcal{V}_{vc}^{\Sigma,a}\{r_{cv'}^b r_{v'v}^c\}]}{2\omega_{cv'}^\Sigma - \omega_{cv}^\Sigma} - \sum_{\mathbf{c}' \neq c} \frac{\text{Im}[\mathcal{V}_{vc}^{\Sigma,a}\{r_{c\mathbf{c}'}^c r_{\mathbf{c}'v}^b\}]}{2\omega_{\mathbf{c}'v}^\Sigma - \omega_{cv}^\Sigma} \right] \delta(\omega_{cv}^\Sigma - 2\omega)$$

Intraband Contribution $\langle n\mathbf{k}|\mathbf{r}_i|m\mathbf{k}'\rangle = \delta_{nm} \left[\delta(\mathbf{k} - \mathbf{k}')\xi_{nn}(\mathbf{k}) + i\nabla_{\mathbf{k}}\delta(\mathbf{k} - \mathbf{k}') \right]$

$$\text{Im}[\chi_{i,\omega}^{\text{abc}}] = \frac{\pi|e|^3}{2\hbar^2} \int \frac{d^3k}{8\pi^3} \sum_{cv} \frac{1}{(\omega_{cv}^\Sigma)^2} \left[\text{Re} \left[\left\{ r_{cv}^b (\mathcal{V}_{vc}^{\Sigma,a})_{;\mathbf{k}^c} \right\} \right] + \frac{\text{Re} [\mathcal{V}_{vc}^{\Sigma,a} \{r_{cv}^b \Delta_{cv}^c\}]}{\omega_{cv}^\Sigma} \right] \delta(\omega_{cv}^\Sigma - \omega)$$

$$\text{Im}[\chi_{i,2\omega}^{\text{abc}}] = \frac{\pi|e|^3}{2\hbar^2} \int \frac{d^3k}{8\pi^3} \sum_{vc} \frac{4}{(\omega_{cv}^\Sigma)^2} \left[\text{Re} \left[\mathcal{V}_{vc}^{\Sigma,a} \left\{ (r_{cv}^b)_{;\mathbf{k}^c} \right\} \right] - \frac{2\text{Re} [\mathcal{V}_{vc}^{\Sigma,a} \{r_{cv}^b \Delta_{cv}^c\}]}{\omega_{cv}^\Sigma} \right] \delta(\omega_{cv}^\Sigma - 2\omega)$$

└ The Nonlinear Surface Susceptibility

└ Software

Medusa runs on free and open source software:

- CentOS 6.7 GNU/Linux
- Intel MPI & OpenMP
- Intel MKL
- Intel FORTRAN & C
- Bash, Perl, Python

TINIBA

Combines Bash, Perl, Fortran, and ABINIT for calculating:

- Optical response of semiconductors
- Optical response of nanomaterials
- Spin injection in materials
- Nonlinear optical response for surfaces and interfaces

└ The Nonlinear Surface Susceptibility

└ Software

ABINIT^{7 8 9}

First-principle study of crystals, molecules, nanostructures using density functional theory, many-body perturbation theory, plane waves, and pseudopotentials to calculate

- Electronic structure
- Total energy
- Dielectric properties, and many, many more

⁷X. Gonze et al. *Computational Materials Science*, 25:478–492, 2002

⁸X. Gonze et al. *Z. Kristallogr.*, 220:558–562, 2005

⁹X. Gonze et al. *Computer Physics Communications*, 180(12):2582, 2009

└ The Nonlinear Surface Susceptibility

└ Software

DP/EXC¹⁰

Linear response time-dependent density-functional theory (LR-TDDFT) code in frequency reciprocal ($\mathbf{k} - \omega$) space on a plane waves (PW) basis set, for dielectric and optical Spectroscopy.

- Optical absorption
- Reflectivity
- Refraction Indices
- EELS

In our case, we use DP for calculating the contribution from \mathbf{v}^{nl} .

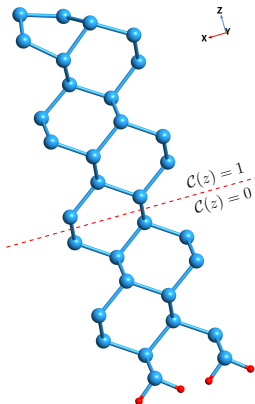
¹⁰Olevano, V. and Reining, L. and Sottile, F., <http://dp-code.org>, <http://etsf.polytechnique.fr/exc/>

└ The Nonlinear Surface Susceptibility

└ Results for χ : Si(001)(2×1)

The Si(001)(2×1) Slab

2×1 reconstruction $\Rightarrow \chi_{2\times 1}^{xxx} \neq 0$



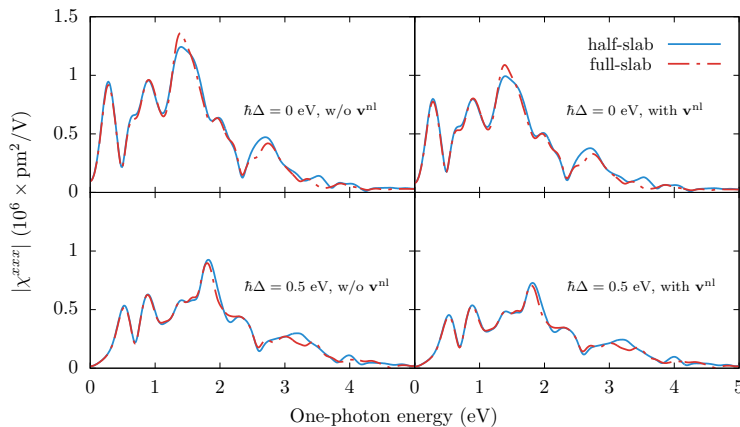
H-terminated $\Rightarrow \chi_H^{xxx} \approx 0$

Convergence is achieved with 32 layers of Si.

└ The Nonlinear Surface Susceptibility

└ Results for χ : Si(001)(2×1)

Half-slab vs. Full-slab

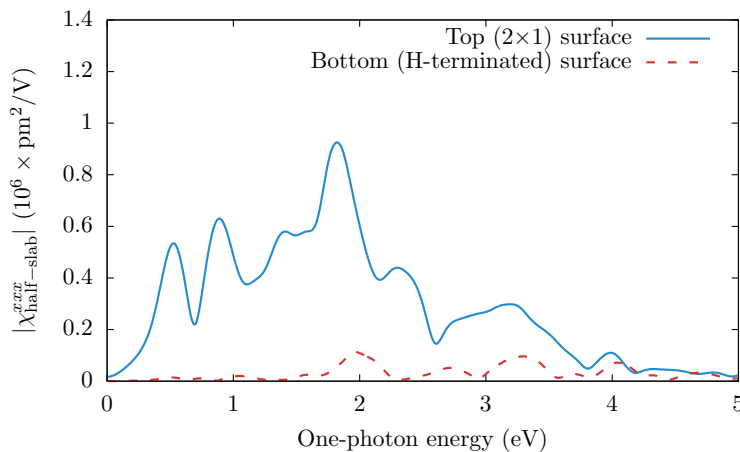


More layers would produce even better results.

└ The Nonlinear Surface Susceptibility

└ Results for χ : Si(001)(2×1)

Top vs. Bottom Surfaces

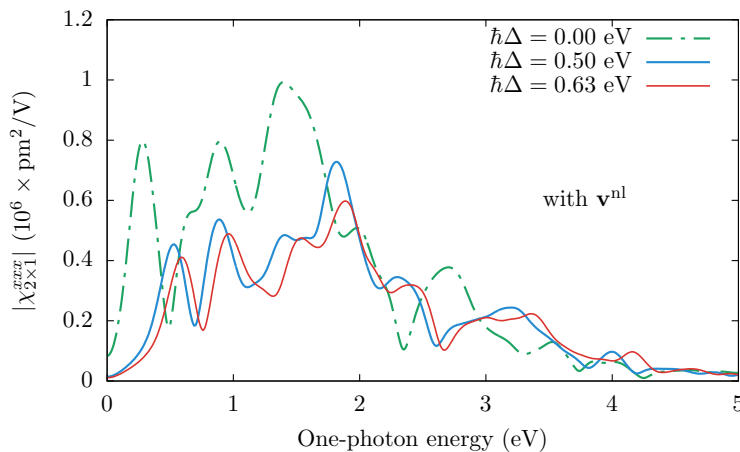


Improved with more layers and more precise division of slab.

└ The Nonlinear Surface Susceptibility

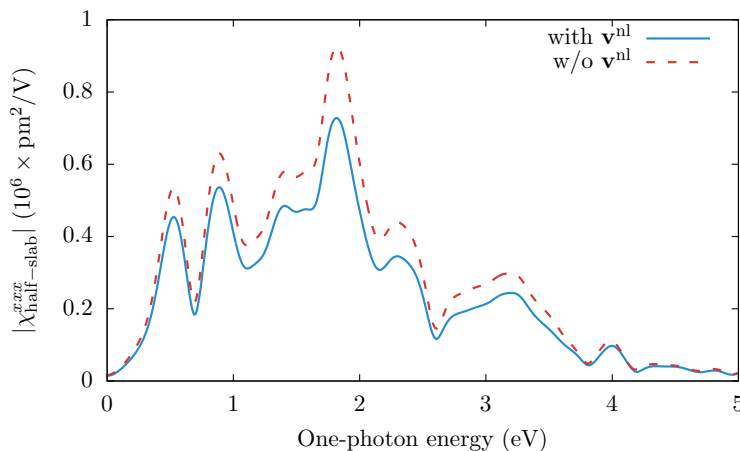
└ Results for χ : Si(001)(2×1)

Three Values of the Scissors Correction



The 2×1 reconstructed surface has surface states, so the spectrum shifts non-rigidly.

└ The Nonlinear Surface Susceptibility

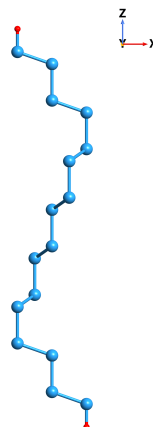
└ Results for χ : Si(001)(2×1)With and Without \mathbf{v}^{nl} 

The effect of the nonlocal part of the pseudopotentials maintains the same line-shape but reduces the value by 15-20% on average.

└ The Nonlinear Surface Susceptibility

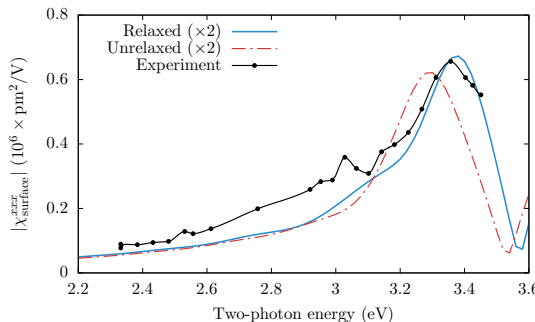
└ Results for χ : Si(111)(1×1):H

The Si(111)(1×1):H surface



Si(111)(1×1):H

└ The Nonlinear Surface Susceptibility

└ Results for χ : Si(111)(1×1):H χ for the Si(111)(1×1):H surface¹¹

Relaxing the Structure

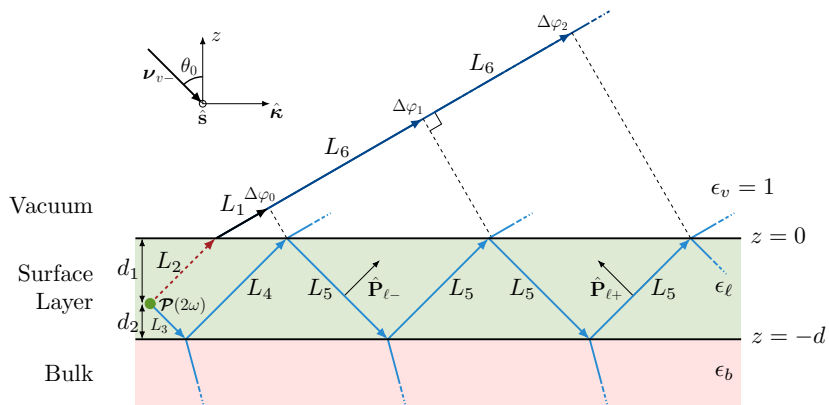
- 1 Worth the time and effort
- 2 Experimental data taken at low temperature

¹¹Experimental data from Höfer et al., Appl. Phys. A 63, 533 (1996)

└ The SSHG Yield

└ Deriving \mathcal{R}

The Three Layer Model



The nonlinear process occurs in a thin layer (ℓ) just below the surface, between the vacuum region (v) and the material bulk (b)

└ The SSHG Yield

 └ Deriving \mathcal{R}

Explicit Expressions for $\mathcal{R}^{12\ 13}$

The SSHG yield is

$$\mathcal{R}_{iF}(2\omega) = \frac{\omega^2}{2\epsilon_0 c^3 \cos^2 \theta_0} \left| \frac{1}{n_\ell} \Upsilon_{iF} \right|^2 \quad \left[\frac{\text{m}^2}{\text{W}} \right]$$

for each combination of polarizations of incoming and outgoing fields ($iF = pP, pS, sP$, and sS). We have that

$$\Upsilon_{iF} = \Gamma_{iF} r_{iF},$$

where,

$$\Gamma_{pP} = \frac{T_p^{v\ell}}{N_\ell} \left(\frac{t_p^{v\ell}}{n_\ell} \right)^2, \quad \Gamma_{sP} = \frac{T_p^{v\ell}}{N_\ell} \left(t_s^{v\ell} r_s^{M+} \right)^2,$$

$$\Gamma_{pS} = T_s^{v\ell} R_s^{M+} \left(\frac{t_p^{v\ell}}{n_\ell} \right)^2, \quad \Gamma_{sS} = T_s^{v\ell} R_s^{M+} \left(t_s^{v\ell} r_s^{M+} \right)^2,$$

¹²Anderson, et al., Phys. Rev. B 93, 235304 (2016)

¹³Anderson, et al., arXiv:1604.07722 (2016)

└ The SSHG Yield

└ Deriving \mathcal{R}

Explicit Expressions for \mathcal{R}

In particular, for the (111) surface we have

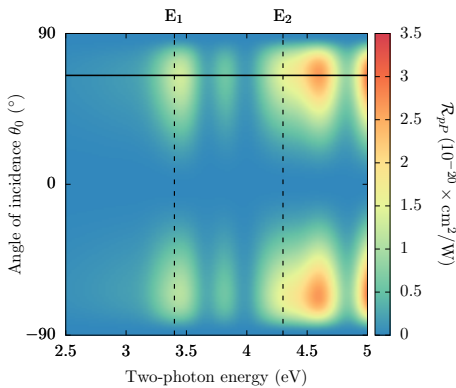
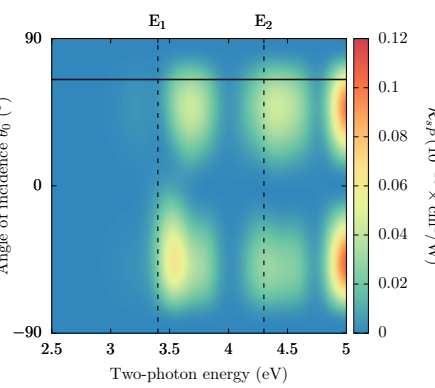
$$\begin{aligned} r_{pP}^{(111)} &= R_p^{M+} \sin \theta_0 \left[\left(r_p^{M+} \right)^2 \sin^2 \theta_0 \chi^{zzz} + \left(r_p^{M-} \right)^2 w_\ell^2 \chi^{zxx} \right] \\ &\quad - R_p^{M-} w_\ell W_\ell \left[2r_p^{M+} r_p^{M-} \sin \theta_0 \chi^{xxz} + \left(r_p^{M-} \right)^2 w_\ell \chi^{xxx} \cos 3\phi \right], \end{aligned}$$

$$r_{sP}^{(111)} = R_p^{M+} \sin \theta_0 \chi^{zxx} + R_p^{M-} W_\ell \chi^{xxx} \cos 3\phi,$$

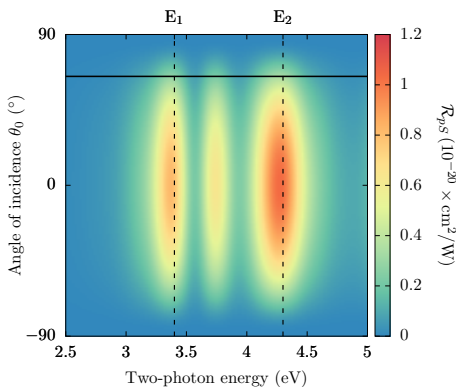
$$r_{pS}^{(111)} = - \left(r_p^{M-} \right)^2 w_\ell^2 \chi^{xxx} \sin 3\phi,$$

$$r_{sS}^{(111)} = \chi^{xxx} \sin 3\phi.$$

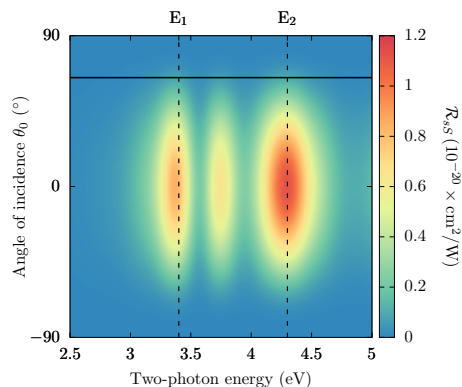
└ The SSHG Yield

└ Results for \mathcal{R} : Si(111)(1×1):HSi(111)(1×1):H – Outgoing P polarization \mathcal{R}_{pP} with $\phi = 45$  \mathcal{R}_{sP} with $\phi = 45$

└ The SSHG Yield

└ Results for \mathcal{R} : Si(111)(1×1):HSi(111)(1×1):H – Outgoing S polarization

\mathcal{R}_{pS} with $\phi = 45$

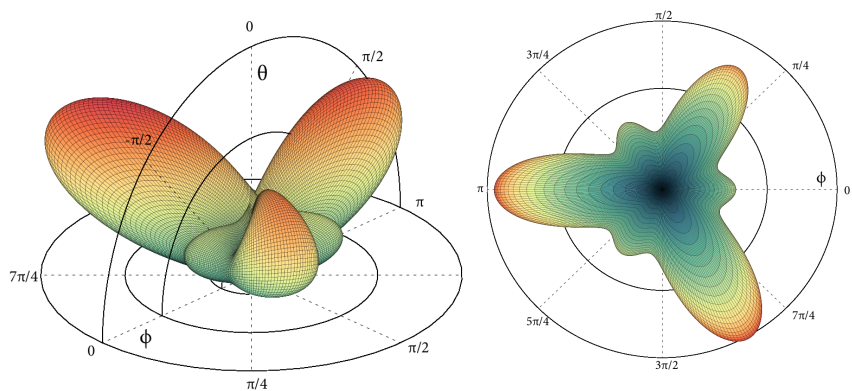


\mathcal{R}_{sS} with $\phi = 45$

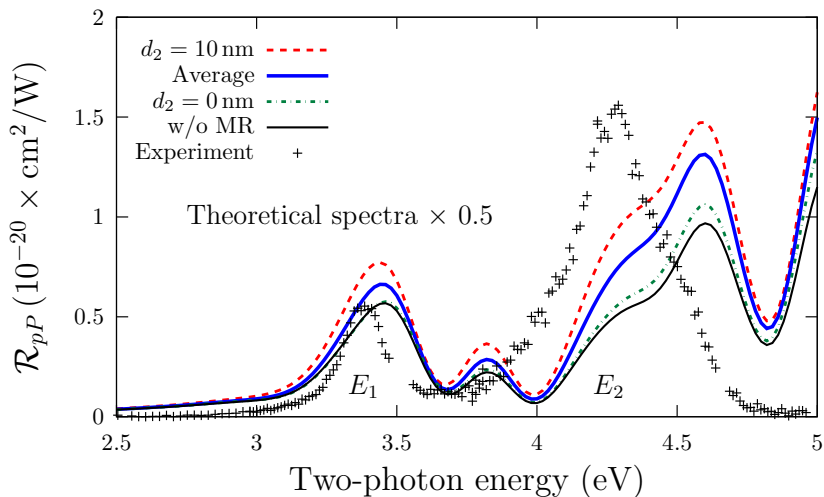
└ The SSHG Yield

└ Results for \mathcal{R} : Si(111)(1×1):H

Si(111)(1×1):H – \mathcal{R}_{pP} at $E_1 = 3.4$ eV



└ The SSHG Yield

└ Results for \mathcal{R} : Si(111)(1×1):H

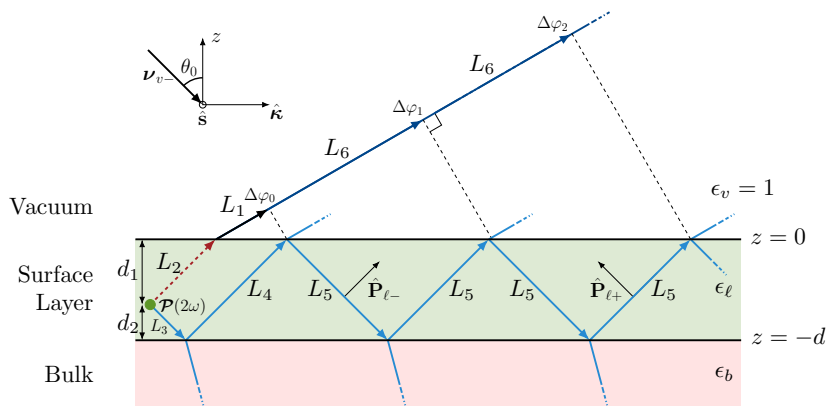
$$\mathcal{R}_{pP} \text{ for } \theta = 65 \text{ and } \phi = 45^{14}$$

¹⁴Experimental data from Mejia et al., Phys. Rev. B 66, 195329 (2002)

└ The SSHG Yield

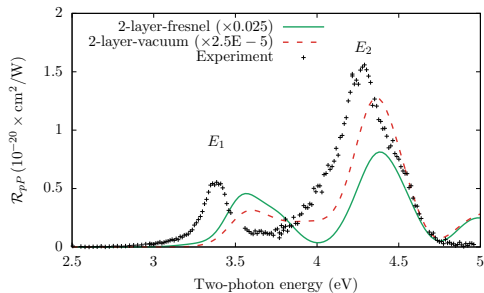
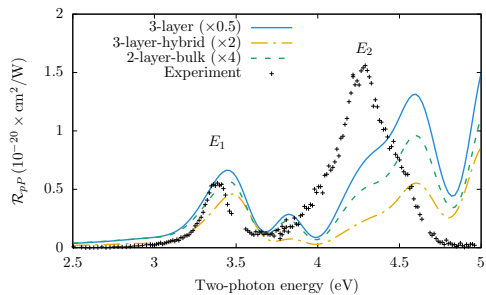
└ Results for \mathcal{R} : Si(111)(1×1):H

The Three Layer Model

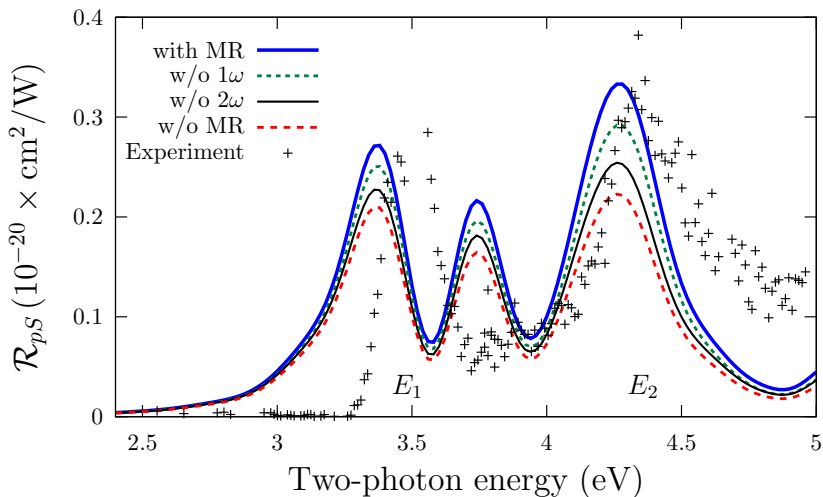


The nonlinear process occurs in a thin layer (ℓ) just below the surface, between the vacuum region (v) and the material bulk (b)

└ The SHHG Yield

└ Results for \mathcal{R} : Si(111)(1×1):H

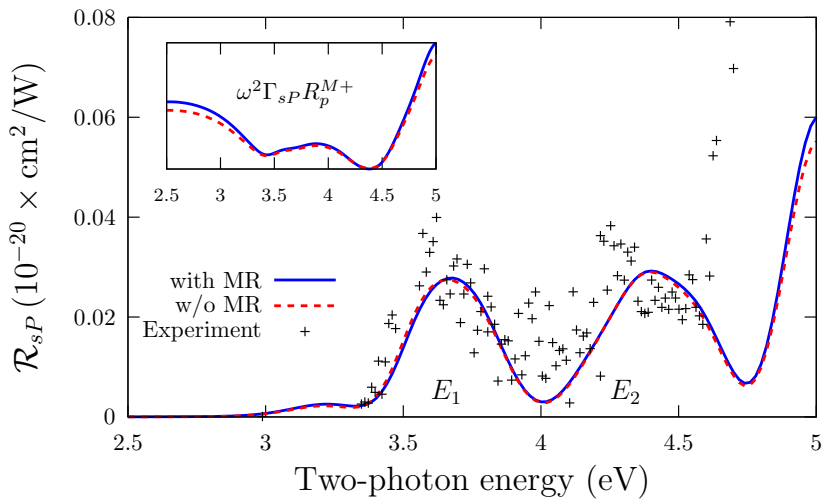
└ The SSHG Yield

└ Results for \mathcal{R} : Si(111)(1×1):H

$$\mathcal{R}_{pS} \text{ for } \theta = 65 \text{ and } \phi = 45^{15}$$

¹⁵Experimental data from Mejia et al., Phys. Rev. B 66, 195329 (2002)

└ The SSHG Yield

└ Results for \mathcal{R} : Si(111)(1×1):H

$$\mathcal{R}_{sP} \text{ for } \theta = 65 \text{ and } \phi = 45^{16}$$

¹⁶Experimental data from Mejia et al., Phys. Rev. B 66, 195329 (2002)

└ The SSHG Yield

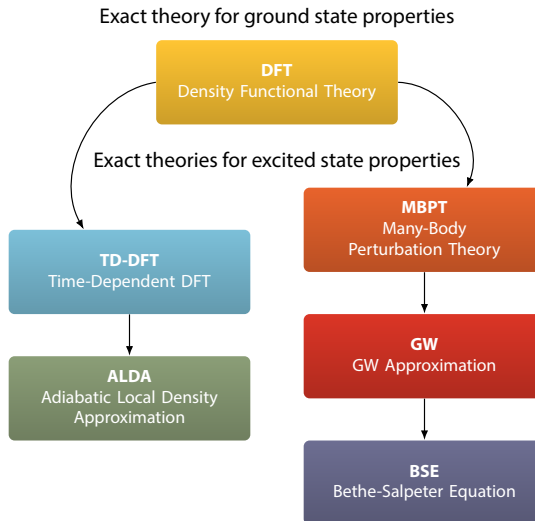
 └ Results for \mathcal{R} : Si(111)(1×1):H

Summary

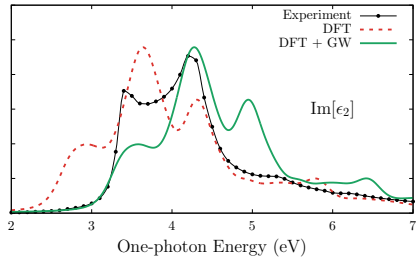
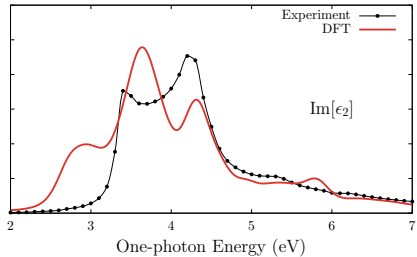
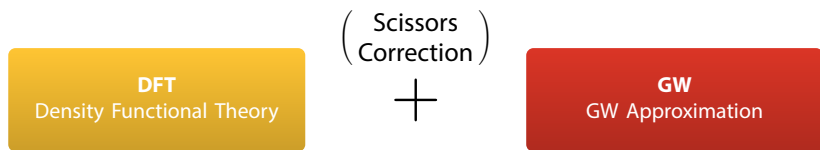
- Intensity is very close to experiment with unambiguous units.
No more AU!
- Peak position is also quite close, temperature effects are quite clear.
- Multiple reflections enhances peak proportions and intensity when needed.
- We can now have *quantitative* and predictive results for any surface!

Remember, this is IPA folks! We neglect excitonic and local field effects.

What's Next?

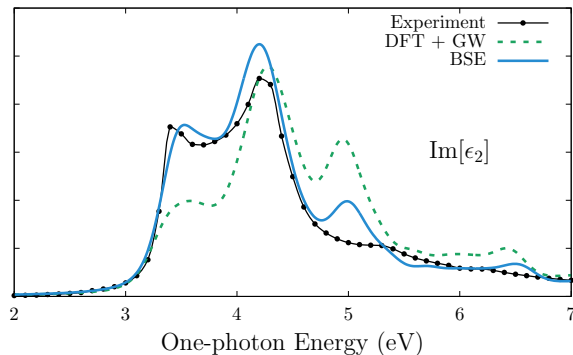


Where We Stand



The State of the Art

BSE
Bethe-Salpeter Equation



Productivity

Produced Articles

- *Anderson, et al.*, Phys. Rev. B 93, 235304 (2016)
- *Zapata-Peña, Anderson, et al.*, Phys. Status Solidi B 253, 408 (2016)
- *Anderson, et al.*, Phys. Rev. B 91, 075302 (2015)
- *Anderson, et al.*, arXiv:1604.07722 [physics.optics] (2016)
- *Anderson, et al.*, Phys. Rev. B, Submitted (2016)

Academic Stays

- Laboratoire des Solides Irradiés, École Polytechnique, France (2015)
- Laboratoire des Solides Irradiés, École Polytechnique, France (2014)

└ Conclusions

└ About Me

Conferences

- Psi-K 2015 (Ganador del Concurso de Posters Científicos)
- OSI-11 2015 (Poster)
- ENU-HPC 2012 (Submitted Talk)

Specialized Courses

- *Ab-initio* calculations with the DP/EXC Codes (2016) (Imparted)
- Control de versiones usando Git y GitHub (2013) (Imparted)
- Cómputo en paralelo mediante FORTRAN/C++ con MPI y OpenMP (2013)
- Cálculo de propiedades ópticas de la materia con el uso de teoría de muchos cuerpos (2013)

Acknowledgements

- Benevolent leader: Dr. Bernardo Mendoza
- Dr. Ramón Carriles Jaimes
- Dr. Norberto Arzate Plata
- Dr. Francisco Villa Villa
- Dr. Wolf Luis Mochán Backal
- The CONACYT
- The CIO for 6 great years

Thanks for coming!